World Journal of Advanced Research and Reviews
eISSN: 2581-9615 CODEN (USA): WJARAI
Cross Ref DOI: 10.30574/wjarr
Journal homepage: https://wjarr.com/

(RESEARCH ARTICLE)

Proteoglycan deposition and Collagen Orientation in Tissue Engineered Cartilage constructs using Digital Densitometry (DD) Imaging and Polarized Light Microscopy (PLM) Techniques

Adekunle Job *

Department of Technical Physics, University of Eastern Finland, Yliopistonranta 8, 70210, Kuopio Finland.

World Journal of Advanced Research and Reviews, 2025, 26(02), 842-855

Publication history: Received on 14 March 2025; revised on 03 May 2025; accepted on 05 May 2025

Article DOI: https://doi.org/10.30574/wjarr.2025.26.2.1344

Abstract

Background: Articular cartilage is an essential connective tissue providing structural integrity and low-friction movement in joints. Due to its avascular nature, its ability to self-repair is limited, necessitating advancements in tissue engineering for cartilage regeneration. The extracellular matrix (ECM) components, primarily proteoglycans and collagen fibers, play a crucial role in determining the biomechanical properties of engineered cartilage. Understanding proteoglycan deposition and collagen orientation is vital for optimizing tissue engineering strategies.

Objective: This study aims to quantify proteoglycan content in histological sections of tissue-engineered cartilage constructs using digital densitometry (DD) imaging and analyze collagen fiber orientation using polarized light microscopy (PLM). Constructs with different cell densities (2M, 5M, and 10M) were evaluated at four time points (Day 1, 7, 14, 21) to assess ECM maturation.

Methods: Tissue-engineered cartilage constructs were cultured using gelatin methacrylic anhydride (GELMA), gellan gum (GG) hydrogel, and scaffold-free (SF) approaches. Histological sections were stained with Safranin-O, and DD imaging was performed using a calibrated Nikon microscope to quantify proteoglycan content. Collagen fiber orientation was analyzed using a Leitz Ortholux II POL microscope at 21 orientations, employing Michelson contrast and anisotropy index calculations for alignment assessment.

Results: Proteoglycan Deposition (DD Imaging): Proteoglycan content increased significantly from Day 14 to Day 21, with scaffold-free constructs exhibiting the highest deposition. Constructs with higher cell densities (5M and 10M) demonstrated greater proteoglycan accumulation compared to lower-density constructs.

Collagen Fiber Orientation (PLM Analysis): Polarized light microscopy revealed that constructs with higher cell densities (5M and 10M) had more organized collagen networks. Scaffold-free constructs exhibited superior collagen alignment compared to hydrogel-based scaffolds. The anisotropy index confirmed increased fiber organization over time, particularly in the 5M and 10M SF groups.

Conclusion: The combination of DD imaging and PLM provided a comprehensive assessment of ECM maturation in tissue-engineered cartilage. The study demonstrated that scaffold-free constructs, particularly those with higher cell densities, exhibited enhanced proteoglycan deposition and superior collagen alignment. These findings support scaffold-free tissue engineering approaches for developing functional cartilage replacements in regenerative medicine.

Future Directions: Further investigations will explore the molecular mechanisms driving ECM organization and optimize scaffold compositions to enhance cartilage regeneration potential for clinical applications.

* Corresponding author: Adekunle Job.

Keywords: PLM; DD; Collagen; GELMA; GG; Proteoglycan

1. Introduction

Articular cartilage is a specialized type of connective tissue that covers the ends of bones within a joint. Its primary function is to provide a smooth, low-friction surface that allows the bones to glide smoothly against each other during joint movement. Articular cartilage is found in synovial joints, which are the most common type of joints in the human body and include joints like the knee, hip, shoulder, and elbow [1-2].

Articular cartilage consists of water (80%), articular cartilage cells (chondrocytes, 2%), and extra-cellular matrix, which includes proteoglycans (40% dry weight) and collagen (60% dry weight) [2]. Unlike other tissues, articular cartilage is avascular, meaning it lacks blood vessels, and aneural, meaning it lacks nerve fibers [2]. This limits its ability to heal and regenerate in response to injuries [2]. Collagen provides structural support, while proteoglycans attract water, giving the cartilage its compressibility and ability to withstand loads [2]. Articular cartilage is often divided into different zones based on its structure and function [2-3]. Matured articular cartilage can be categorized into four distinct zones based on the collagen fibril orientation; the superficial, middle, deep, and calcified cartilage zones [3]. In the superficial zone, the collagen fibrils (type II and type IX) are oriented parallel to the articular surface. In the middle zone, the fibril orientation is irregular (random orientation) due to the transition from parallel orientation at the tissue surface to perpendicular orientation at the deep cartilage. In the deep zone, the orientation is perpendicular to the surface of the articular cartilage; while for the calcified cartilage zones, the cartilage connects to the subchondral bone [1-2]. In the extra cellular matrix (ECM), collagen is the most prevalent structural macromolecule; it accounts for around 60% of cartilage's dry weight. 90% to 95% of the collagen in the extracellular matrix (ECM) is type II collagen, which forms fibrils and fibers entwined with proteoglycan aggregates. Although present, collagen types I, IV, V, VI, IX, and XI make up a small part of the total. The type II collagen fibril network is formed and stabilized with the aid of the minor collagens [2].

Collagen type II forms the elementary component of the cross branded fibrils. While collagen type XI molecule bind covalently to collagen type II molecules and possibly become part of the interior structure of the cross banded fibrils. However, the functions of collagen type IX and type XI remain unclear. Nevertheless, it is assumed that they assist to stabilize and form the collagen fibrils collected fundamentally from collagen type II. The collagen type IX molecules extended portions can help bind the collagen fibril meshwork and interact with collagen meshwork with proteoglycans. Collagen type VI look to form a vital portion of the matrix, surrounding the chondrocytes and aids the attachment of the chondrocytes to the matrix. Collagen type X presence only close to the cells of the calcified zone of articular cartilage and the hypertrophic zone of growth plate that is the area where the longitudinal cartilage septa begin to mineralize, thereby suggests that type X has a part in cartilage militarization [5].

Proteoglycans play a crucial role in the structure and function of cartilage, particularly in articular cartilage found in joints. They are a type of macromolecule consisting of a core protein and long chains of carbohydrates called glycosaminoglycans (GAGs). Proteoglycans contribute to the unique properties of cartilage, such as its ability to resist compressive forces and retain water [7]. Here's how proteoglycan deposition works in cartilage.

When pressure is applied to the joint, water within the proteoglycan-rich matrix is squeezed out, and as pressure is released, water is drawn back in, helping the cartilage return to its original shape [5]. This mechanism is crucial for shock absorption and joint lubrication [5]. In conditions like osteoarthritis, the balance between proteoglycan synthesis and degradation can be disrupted, leading to a loss of proteoglycans and deterioration of cartilage [5]. Researchers are investigating strategies to promote proteoglycan synthesis and repair damaged cartilage, including tissue engineering and regenerative therapies.

Tissue engineering is a multidisciplinary field that aims to create functional and viable tissues or organs using a combination of cells, biomaterials, and bioactive molecules [9].

The primary component of TE, scaffolds, promote tissue regeneration by fostering an environment that is conducive to cell anchoring, distribution, and functionalization in the presence of signaling molecules [10].

Cartilage tissue engineering aims to create functional cartilage replacements for damaged or degenerated cartilage in joints, such as in cases of osteoarthritis [9]. In tissue engineering, bio-material scaffolds are used to support cell growth and guide tissue formation. These scaffolds often mimic the natural extracellular matrix of the tissue being engineered. For cartilage tissue engineering, scaffolds are designed to support the deposition of proteoglycans, collagen, and other

components present in native cartilage [10]. While independent methods do not rely on scaffolds, scaffold-dependent procedures employ synthetic or natural biomaterials to create an environment that encourages cell development and interactions [4].

Scaffolds made of hydrogel are becoming a common therapy option for cartilage abnormalities. They are minimally invasive, replicate the natural environment, and may be injected to fill irregularly shaped lesions. Although initial mechanical stability is a key attribute of scaffolds, they come with a number of disadvantages, including cell-characteristic changes, remodeling resistance, stress shielding, and toxicity associated with degradation [4]. When creating cartilage tissue using tissue engineering approaches, chondrocytes (cartilage cells) or stem cells are seeded onto the scaffolds. Over time, these cells proliferate and differentiate into chondrocyte-like cells that deposit proteoglycans and collagen, forming a tissue-engineered cartilage matrix [9]. Growth factors and bioactive molecules can be incorporated into tissue engineering approaches to enhance proteoglycan deposition and tissue maturation. These factors can stimulate chondrogenic differentiation and promote the synthesis of proteoglycans by the cultured cells [9].

The successful outcome of tissue engineering relies on the maturation of the engineered tissue to closely resemble native tissue [9]. Proteoglycan content and distribution are important markers for assessing the maturity and functionality of tissue-engineered cartilage [9].

Staining articular cartilage sections with Safranin O is a common method used to visualize the presence of glycosaminoglycans (GAGs), which are a major component of the cartilage extracellular matrix. Safranin O is a cationic dye that binds to the negatively charged GAGs, staining them red [11]. The intensity of red staining corresponds to the number of GAGs present in the cartilage matrix [11]. Regions with higher GAG content will appear darker red [11]. GAGs are abundant in the extracellular matrix of cartilage, particularly in areas rich in proteoglycans, such as the territorial matrix around chondrocytes and the inter-territorial matrix. You would observe red staining in these areas [11]. In cases of cartilage degeneration or damage, such as osteoarthritis, there might be a reduced presence of GAGs. This would result in reduced or absent Safranin O staining in the affected areas [12].

Digital densitometry is a technique used in various fields, including radiology, astronomy, and materials science, to measure the density or optical density of a material or substance. It involves the use of digital imaging technology and software to analyze the attenuation or absorption of light or other electromagnetic radiation as it passes through or interacts with a sample. The digital aspect of densitometry involves using digital sensors or cameras to capture images, followed by computer-based analysis to calculate the optical density values.

Polarized light microscopy is a traditional technique for visualizing the collagen network structure of articular cartilage. Articular cartilage repair and tissue engineering researches have evolved new request for techniques with capacity of quantitative characterization of the scar and repair tissues, as well as properties of the collagen network. Modern polarized light microscopy can be used to analyze parallelism,birefringence and collagen fibril orientation. Modern instruments are computer based and the measurements are more flexible to perform. Nevertheless, on many numerous occasions the presentation of results brings about difficulties, even errors, due to the demand in the theoretical aspects of the technique [20]. Prior to each PLM measurement session, automated alignment and calibration procedures are run to guarantee measurement reliability. Following alignment, the microscope is calibrated. Calculating the sample's orientation-dependent birefringence required this calibration technique. For impartial study of fibril parallelism or orientation, it is not required. After the polarizer has been rotated step-by-step, grayscale photos are taken. The device will continue to capture photos until the camera's saturation point is achieved [20].

1.1. Objective of the study

The objective of this project work is to get familiar with Quantifying proteoglycan (PG) content concentration in histology sections of three types of tissue engineered cartilage constructs with digital densitometry (DD) imaging techniques, and observing the difference in these biomarkers to demonstrate the influence of these gels and scaffold free on the developing neo-tissue. While the polarized light microscopy (PLM) will be used to study collagen fibers orientation, where the polarization direction of the light is affected by the collagen fibers.

2. Material and Method

In this project, there were three types of tissue engineered cartilage constructs which include number of cells (2M, 5M and 10M), and each construct were cultured for four different durations (Day 1, 7, 14 and 21). These tissue constructs were prepared using bone marrow mesenchymal stem cells (BMSCs) encapsulated in gelatin methacrylic anhydride

(GELMA) (n=16) and gellan gum (GG) hydrogel (n=16) or suspended in the media as pellets (scaffold-free constructs; n=16). These constructs were recovered at four time points (Day 1, 7, 14, 21; n=4/gel/time point) and frozen till the beginning of the project.

A set of histological sections were prepared to study PG deposition from frozen samples. The samples were thawed and used to prepare histology sections. This set of histological section were stained using Safranin-o (n=2/gel/time point), a substance that make the proteoglycan to become visible with a reddish color and this was used for Digital Densitometry (DD), where the concentration of safranin-o correlates to the deposition of PG in the samples.

Digital densitometry imaging was acquired with a light microscope (Nikon Microphot FXA, Tokyo, Japan) equipped with a CCD-cooled camera (Hamamatsu photonics K.K, Hamamatsu City, Japan, pixel size = 0.14 lm) and 4x and 10x magnification. Images were calibrated against neutral density filters (optical density values 0.0, 0.3, 0.6, 1.0, 1.3, 1.6, 2.0, 2.6, and 3.0) (Schott, Mainz, Germany). Calibration images were taken at every day before DD measurement for different configuration.

Each sample were indicated with a symbol M, SP, SF which represent GELMA, gellan gum and scaffold free respectively, and each of the samples were seeded with cells in the range from cell free to, 2 million, 5 million, and 10 million cells. Three slices per sample were measured. The data obtained from these measurements provided information on the tissue-engineered cartilage. The image data obtained from DD is processed using MATLAB. The results obtained will also be used as preliminary data for future studies.

The Leitz Ortholux II POL (Leitz Wetzlar, Wetzlar, Germany) microscope body was used for this study's enhanced polarised light microscopy (PLM) instrument, which was calibrated in accordance with Mehta et al. [18]. It was equipped with a monochromatic light source (λ = 630 nm, Edmund Optics Inc., Barrington, NJ, USA), crossed polarizers (Techspec optics A sample is positioned at a 90-degree angle between a polarizer and an analyzer in the set-up. Samples were measured at 21 orientations spanning 180 degrees, spaced 9 degrees apart.

MATLAB program was used for all the analyses to determine the orientation of collagen fibers (Matlab R2023a, Mathworks Inc., Natick, USA).

The fibrous collagen network structure of articular cartilage imposes an angle dependence on the intensity of the observed light. Thus, by measuring the sample at several angles, a parallelism index (i.e., anisotropy) can be defined using Michelson contrast [19]. This type of linear polarization enabled the use of Stokes parameters (S_0, S_1, and S_2) in the calculation of the mean fiber angle in each pixel.

$$S_0 = I(0°) + I(90°), S_1 = I(0°) - I(90°), S_2 = 2 \times I(45°) - S_0 \quad \text{..... (1)}$$

Where I: light/signal intensity in each pixel at the specified polarization angle, S_0: total intensity of incident light, S_1: the amount of linear/horizontal polarization, and S_2: the amount of +45° or -45° polarization. The angle of collagen fibers (ψ) is the orientation of the birefringent structures (i.e., collagen fibers):

$$\psi = \frac{arctan\left(\frac{S_2}{S_1}\right)}{2} \quad \text{..... (2)}$$

Where $0° \leq \psi \leq 90°$ (3). After acquiring the PLM image of the sections, the collagen orientation was estimated on a pixel-by-pixel basis.

3. Result

3.1. Digital Densitiometry (DD) Result

In this result proteoglycan deposition in tissue engineered cartilage constructs were analyzed. This was done in histology sections of three types of tissue engineered cartilage contracts with digital densitometry (DD) imaging techniques using magnification 4 and 10. The proteoglycan content based of these magnifications and the days of culture which are day 14 and 21 were compared. Data for day 1 and 7 were inaccessible due to the small sizes of our samples and difficultly to prepare histology slides which make it difficult to have a reasonable result on those days.

Table 1 and 5 (fig. 1 and fig. 5) are used to show day 14 and 21 for comparison for all amount of cells in both magnification 4 and 10 respectively and while table 2 and 6 (fig. 2 and fig. 6), table 3 and 7 (fig 3 and fig.7) and table 4 and 8 (fig. 4 and fig. 8) are used for day 14 and 21 for comparison with amount of cells 2M, 5M and 10M respectively in both magnification 4 and 10.

Table 1 Average values of proteoglycan for day 14 and 21 (Mag. 4)

4X Day 14	average	4X Day 21	average
0M_DAY14_B1	0.1725	0M_DAY21_A1	0.1142
10M_DAY14A_A1	0.2878	0M_DAY21_B1	0.4554
10M_DAY14B_A1	0.2012	0M_DAY21_C1	0.1946
10SF_DAY14_A1	0.1789	10M_DAY21_A1	0.1562
10SF_DAY14_B1	0.1334	10M_DAY21A_B1	0.2275
10SP_DAY14_A1	0.0960	10M_DAY21B_B1	0.2446
10SP_DAY14_B1	0.0893	10SF_DAY21_A1	0.3774
2M_DAY14A_A1	0.1909	10SF_DAY21_B1	0.2325
2M_DAY14A_B1	0.1137	10SP_DAY21A_A1	0.0572
2M_DAY14B_A1	0.0822	10SP_DAY21B_A1	0.0606
2M_DAY14B_B1	0.1244	2M_DAY21A_A1	0.1049
2SF_DAY14_A1	0.1965	2M_DAY21B_A1	0.1545
2SF_DAY14_B1	0.1944	2M_DAY21B_B1	0.2734
5M_DAY14_A1	0.1559	2SF_DAY21_A1	0.2339
5M_DAY14A_B1	0.1156	5M_DAY21_A1	0.1695
5SF_DAY14_A1	0.1412	5M_DAY21A_B1	0.1665
5SF_DAY14_B1	0.2681	5M_DAY21B_B1	0.1606
		5SF_DAY21_A1	0.4866
		5SF_DAY21_B1	0.2865

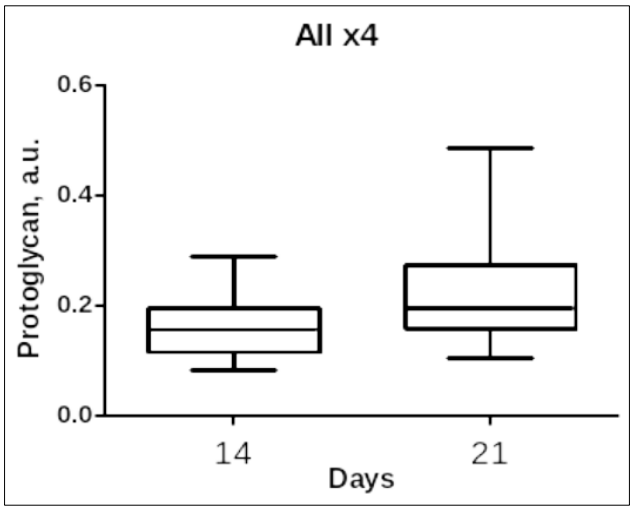

Figure 1 The plot of day 21 and day 14 (mag. 4)

The plot simple revealed the abundance of proteoglycan in day 21 in comparison with day 14 and the mid values in day 21 is thicker than that of day 14, the mid values as seen still confirmed the greater concentration of proteoglycan in day 21 to day 14.

Table 2 Average values of proteoglycan for 2million cells scaffold (Mag. 4)

day 14	average	day 21	average
2M_DAY14A_A1	0.1909	2M_DAY21A_A1	0.1049
2M_DAY14A_B1	0.1137	2M_DAY21B_A1	0.1545
2M_DAY14B_A1	0.0822	2M_DAY21B_B1	0.2734
2M_DAY14B_B1	0.1244	2SF_DAY21_A1	0.2339
2SF_DAY14_A1	0.1965		
2SF_DAY14_B1	0.1944		

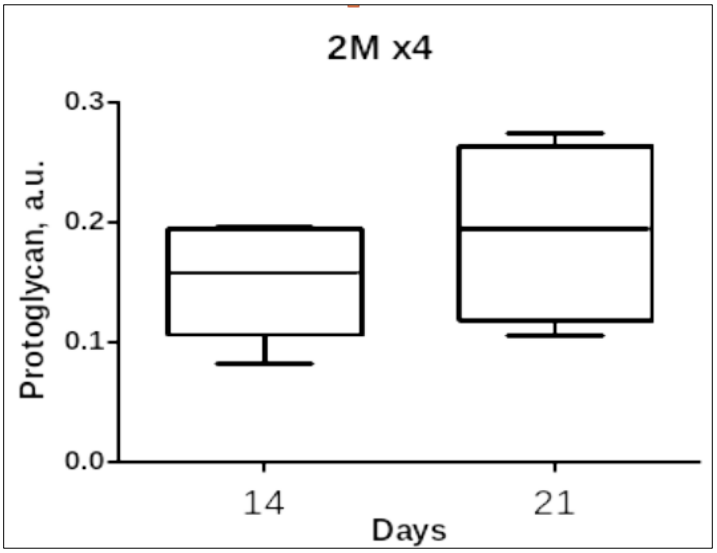

Figure 2 The plot of day 21 and day 14 in 2million cells scaffold (mag. 4)

The plot still revealed the superiority of day21 with the content of proteoglycan side by side to day 14 in 2 million cells scaffold and the mid values in day 21 still thicker than that in day 14, this also confirmed the level of proteoglycan content higher in day 21.

Table 3 Average values of proteoglycan for 5million cells scaffold (Mag. 4)

day 14	average	day 21	average
5M_DAY14_A1	0.1559	5M_DAY21_A1	0.1695
5M_DAY14A_B1	0.1156	5M_DAY21A_B1	0.1665
5SF_DAY14_A1	0.1412	5M_DAY21B_B1	0.1606
5SF_DAY14_B1	0.2681	5SF_DAY21_A1	0.4866
		5SF_DAY21_B1	0.2865

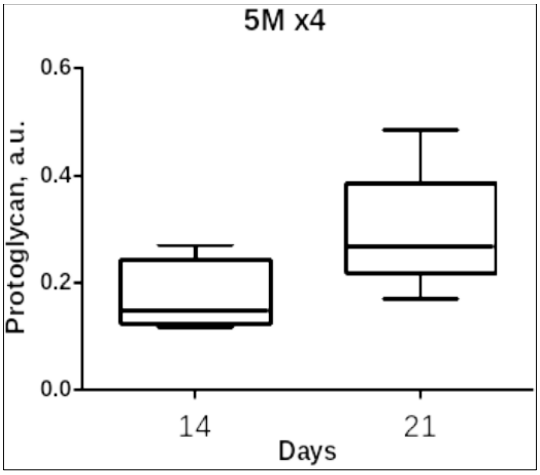

Figure 3 The plot of 5million cells scaffold (mag. 4)

Day 21 with the content of proteoglycan high than day 14 in 5 million cells scaffold and the mid values in day 21 still thicker, this also confirmed the level of proteoglycan content higher in day 21.

Table 4 Average values of proteoglycan for 10million cells scaffold (Mag 4)

day 14	average	day 21	average
10M_DAY14A_A1	0.2878	10M_DAY21_A1	0.1562
10M_DAY14B_A1	0.2012	10M_DAY21A_B1	0.2275
10SF_DAY14_A1	0.1789	10M_DAY21B_B1	0.2447
10SF_DAY14_B1	0.1334	10SF_DAY21_A1	0.3774
10SP_DAY14_A1	0.0960	10SF_DAY21_B1	0.2325
10SP_DAY14_B1	0.0893	10SP_DAY21A_A1	0.0572
		10SP_DAY21B_A1	0.0606

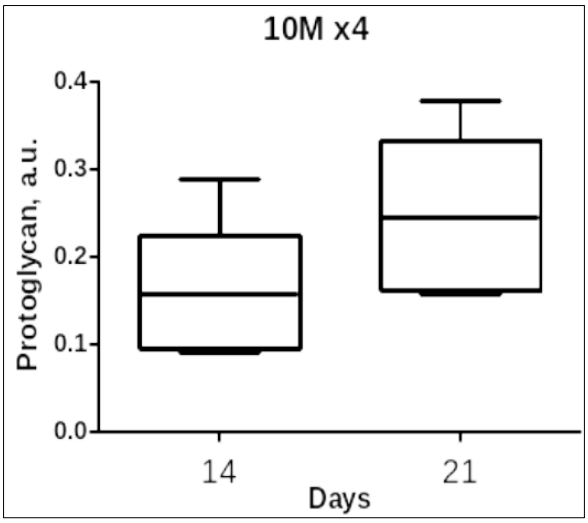

Figure 4 The plot of 5 million cells scaffold (magnification 4)

This plot remains consistent with others showing the consistency of day 21 having high proteoglycan compared to day 14.

Table 5 Average values of proteoglycan for day 14 and 21 (Mag.10)

10X DAY 14	average	10X DAY 21	average
10 M_DAY14A_A1	0.2173	0M_DAY21_B1	0.1526
10 M_DAY14A_B1	0.1775	0M_DAY21_C1	0.2364
10 M_DAY14B_A1	0.2420	0M_DAY21A_AI	0.2300
10 M_DAY14B_B1	0.1633	0M_DAY21B_A1	0.2074
10SF_DAY14_A1	0.1970	0SP_DAY21_A1	0.6755
10SF_DAY14_B1	0.3785	10M_DAY21_A1	0.1279
10SP_DAY14_A1	0.1143	10M_DAY21A_B1	0.2496
10SP_DAY14_B1	0.2170	10M_DAY21B_B1	0.2100
2M_DAY14_A1	0.1778	10SF_DAY21_B1	0.2430
2M_DAY14_B1	0.1744	10SF_DAY21A_A1	0.3678
2SF_DAY14_A1	0.2053	10SF_DAY21B_A1	0.3598
2SF_DAY14_B1	0.2121	10SP_DAY21_A1	0.0955
5M_DAY14_A1	0.1834	2M_DAY21_B1	0.1596
5M_DAY14_B1	0.1782	2M_DAY21A_A1	0.2752
5SF_DAY14_A1	0.1497	2M_DAY21B_A1	0.1622
5SF_DAY14_B1	0.2914	2SF_DAY21_A1	0.2456
		5M_DAY21_A1	0.4860
		5M_DAY21A_B1	0.2189
		5M_DAY21B_B1	0.2238
		5SF_DAY21_A1	0.4014
		5SF_DAY21_B1	0.2415

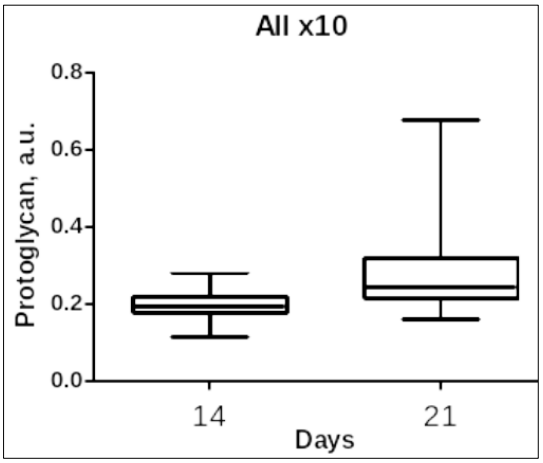

Figure 5 The plot of day 21 and day 14 (mag.10)

The plot revealed the abundance of proteoglycan on day 21 in comparison with day 14 and the mid values in day 21 and day 14, however look similar in thickness, but the day 21 remain high in proteoglycan content.

Table 6 Average values of proteoglycan for 2-day million cells scaffold (Mag.10)

day 14	average	day 21	average
2M_DAY14_A1	0.1778	2M_DAY21_B1	0.1596
2M_DAY14_B1	0.1744	2M_DAY21A_A1	0.2752
2SF_DAY14_A1	0.2053	2M_DAY21B_A1	0.1622
2SF_DAY14_B1	0.2121	2SF_DAY21_A1	0.2456

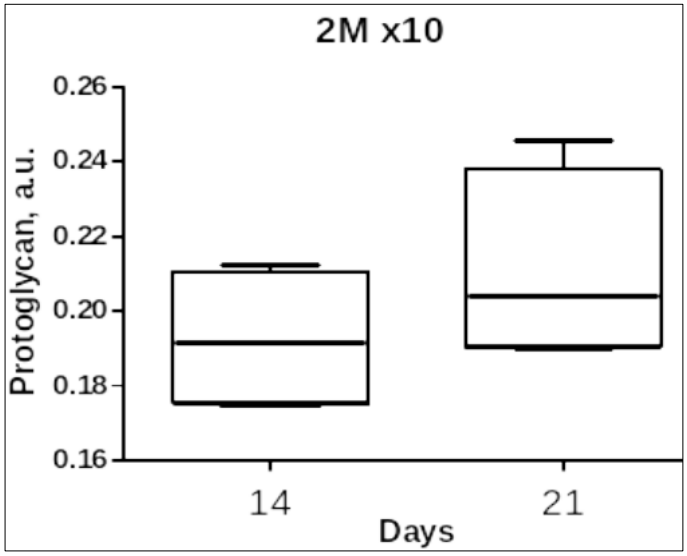

Figure 6 The plot of day 21 and day 14 in 2million cells scaffold (mag.10)

The plot still revealed the superiority of day21 with the content of proteoglycan side by side to day 14 in 2million cells scaffold and the mid values in day 21 still thicker than that in day 14, this also confirmed the level of proteoglycan content higher in day 21.

Table 7 Average values of proteoglycan for 5million cells scaffold (Mag. 10)

day 14	average	day 21	average
5M_DAY14_A1	0.1834	5M_DAY21_A1	0.4860
5M_DAY14_B1	0.1782	5M_DAY21A_B1	0.2189
5SF_DAY14_A1	0.1497	5M_DAY21B_B1	0.2238
5SF_DAY14_B1	0.2914	5SF_DAY21_A1	0.4014
		5SF_DAY21_B1	0.2415

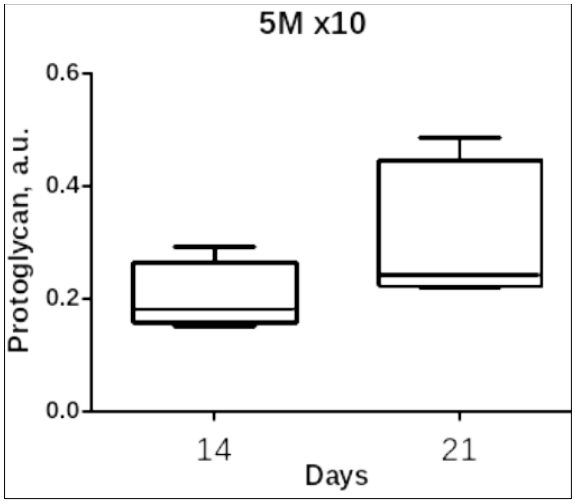

Figure 7 The plot of 5million cells scaffold (mag.10)

Day21 with the content of proteoglycan high than day 14 in 5million cells scaffold and the mid values in day 21 still thicker and higher, this also confirmed the level of proteoglycan content higher in day 21

Table 8 Average values of proteoglycan for 10million cells scaffold (Mag.10)

day 14	average	day 21	average
10 M_DAY14A_A1	0.2173	10M_DAY21_A1	0.1279
10 M_DAY14A_B1	0.1775	10M_DAY21A_B1	0.2496
10 M_DAY14B_A1	0.2420	10M_DAY21B_B1	0.2100
10 M_DAY14B_B1	0.1633	10SF_DAY21_B1	0.2430
10SF_DAY14_A1	0.1970	10SF_DAY21A_A1	0.3678
10SF_DAY14_B1	0.3785	10SF_DAY21B_A1	0.3598
10SP_DAY14_A1	0.1143	10SP_DAY21_A1	0.0955
10SP_DAY14_B1	0.2170		

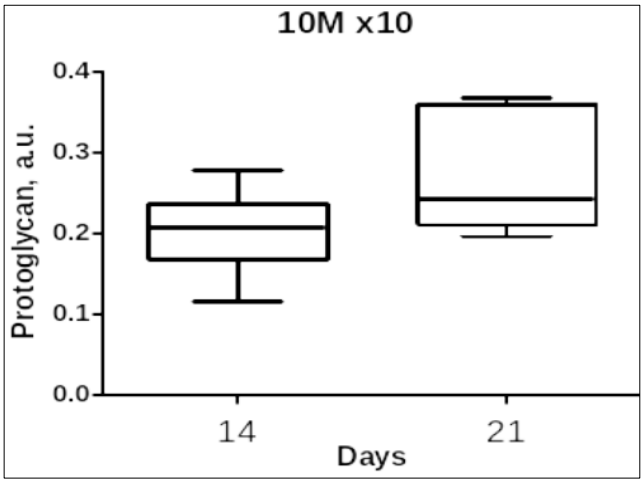

Figure 8 The plot of 5 mmillion cells scaffold (mag.10)

This plot remains consistent that proteoglycan in day 21 is higher than the one in day 14.

Table 9 and 10 (fig. 9 (a and b)) and table 11 and 12 (fig.10 (a and b)) below were used to compare the cells deposited in each scaffold, 2M, 5M and 10M irrespective of days to determine their proteoglycan content in both magnification 4 and 10.

Table 9 Average values of proteoglycan for 2, 5 and 10 million cells scaffold Day 14 (Mag. 4)

		Day 14 4X			
	average		**average**		**average**
2M_DAY14A_A1	0.1909	5M_DAY14_A1	0.1559	10M_DAY14A_A	0.2878
2M_DAY14A_B1	0.1137	5M_DAY14A_B1	0.1156	10M_DAY14B_A1	0.2012
2m_DAY14B_A1	0.0822	5SF_DAY14_A1	0.1412	10SF_DAY14_A1	0.1789
2M_DAY14B_B1	0.1244	5SF_DAY14_B1	0.2681	10SF_DAY14_B1	0.1334
2SF_DAY14_A1	0.1965			10SP_DAY14_A1	0.0960
2SF_DAY14_B1	0.1944			10SP_DAY14_B1	0.0893

Table 10 Average values of proteoglycan for 2, 5 and 10 million cells scaffold Day 21 (Mag. 4)

		Day 21 4X			
	average		**average**		**average**
2M_DAY21A_A1	0.1049	5M_DAY21_A1	0.1695	10M_DAY21_A1	0.1562
2M_DAY21B_A1	0.1545	5M_DAY21A_B1	0.1665	10M_DAY21A_B1	0.2275
2M_DAY21B_B1	0.2734	5M_DAY21B_B1	0.1606	10M_DAY21B_B1	0.2447
2SF_DAY21_A1	0.2339	5SF_DAY21_A1	0.4866	10SF_DAY21_A1	0.3774
		5SF_DAY21_B1	0.2865	10SF_DAY21_B1	0.2325
				10SP_DAY21A_A1	0.0572
				10SP_DAY21B_A1	0.0606

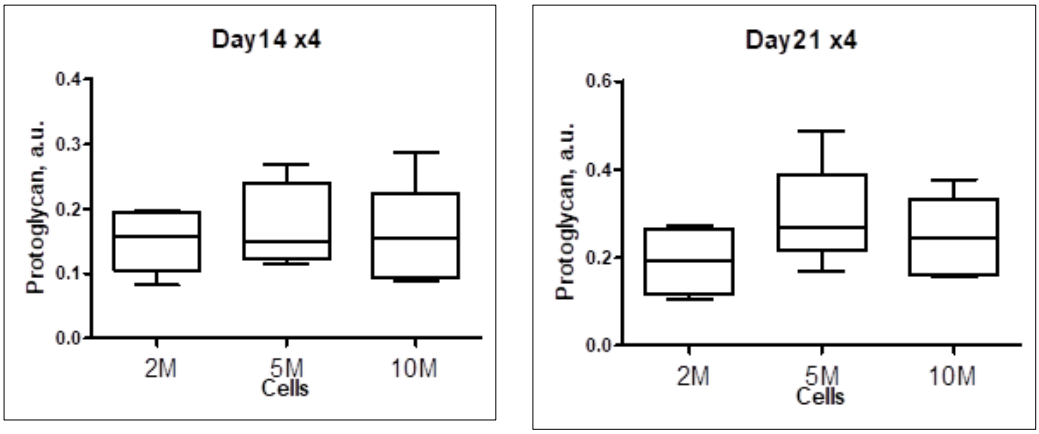

Figure 9 The plot of 2, 5 and 10 million cells scaffold Day 14(a) and 21(b) (mag. 4)

It is seen that in this plot that scaffold with 5M cells gave the highest content of proteoglycan compared to 2M and 10M cells respectively.

Table 11 Average values of proteoglycan for 2, 5 and 10 million cells scaffold Day 14 (Mag. 10)

		Day 14 10X			
	average		**average**		**average**
2M_DAY14_A1	0.1778	5M_DAY14_A1	0.1834	10 M_DAY14A_A1	0.2173
2M_DAY14_B1	0.1744	5M_DAY14_B1	0.1782	10 M_DAY14A_B1	0.1775
2SF_DAY14_A1	0.2053	5SF_DAY14_A1	0.1497	10 M_DAY14B_A1	0.2420
2SF_DAY14_B1	0.2121	5SF_DAY14_B1	0.2914	10 M_DAY14B_B1	0.1633
				10SF_DAY14_A1	0.1970
				10SF_DAY14_B1	0.3785
				10SP_DAY14_A1	0.1143
				10SP_DAY14_B1	0.2170

Table 12 Average values of proteoglycan for 2, 5 and 10 million cells scaffold Day 21(Mag. 10)

		Day 21 10X			
	average		**average**		**average**
2M_DAY21_B1	0.1596	5M_DAY21_A1	0.4860	10M_DAY21_A1	0.1279
2M_DAY21A_A1	0.2752	5M_DAY21A_B1	0.2189	10M_DAY21A_B1	0.2496
2M_DAY21B_A1	0.1622	5M_DAY21B_B1	0.2238	10M_DAY21B_B1	0.2100
2SF_DAY21_A1	0.2456	5SF_DAY21_A1	0.4014	10SF_DAY21_B1	0.2430
		5SF_DAY21_B1	0.2415	10SF_DAY21A_A1	0.3678
				10SF_DAY21B_A1	0.3598
				10SP_DAY21_A1	0.0955

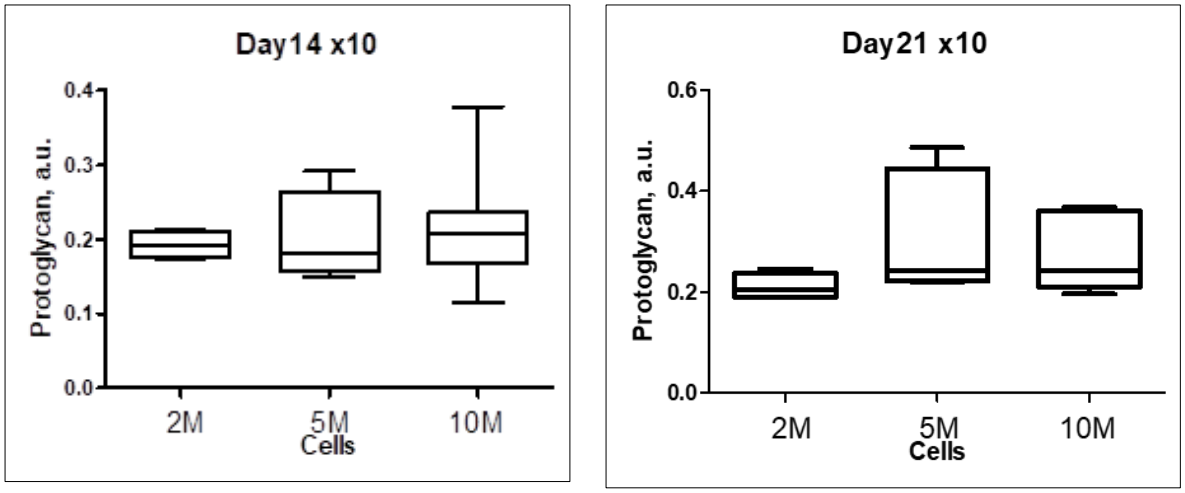

Figure 10 The plot of 2, 5 and 10 million cells scaffold Day 14 (a) and 21(b) (mag. 10)

The same as seen with the previous, it showed that 5M cells scaffold remain consistent, having the highest content of proteoglycan when compared vis a vis to 2M and 10M cells scaffold.

4. Conclusion

This project was anchored to show the level of proteoglycan in a cultured cells on scaffolds, and scaffold free in their millions (2, 5 and 10), to ascertain the level of proteoglycan in the days in which they were cultured which are day 1, 7 , 14 and 21 using Digital Densitometry (DD) imaging techniques. However, day 1 and 7 could not actually give valuable data to work with and a decision was taken to work with day 14 and 21. Viewing the above results, we decide to use the average and the mid value gotten after analyzing the data from the DD techniques with Matlab. The result simply shows a consistent trend, given that 5M cells revealed most proteoglycan concentration in respective of the day under analysis. It is showed that the increase in the number of days for culturing increases the level of proteoglycan while it is seen that several of the cells dies as the day of cultured increases. The result also revealed that increase in the number of cells such as 10 million do not validate the increase or concentration of proteoglycan in the data. We used magnification 4 and 10 to validate our results due to the exceedingly small size of cultured cells we were able to get which affected the result on day 1 and 7 as previously mentioned above. However, the results from magnification 4 and 10 showed similar trends. The result shows that the increase in proteoglycan levels in cultured cells is determined by the number of cells attached to the scaffold and the number of days in culture. The result of this project will be used for optimization of tissue engineered cartilage constructions.

References

[1] Rieppo, L. et al. (2016) Vibrational spectroscopy of articular cartilage. Applied Spectroscopy Reviews. [Online] DOI: 10.1080/05704928.2016.1226182.

[2] Sophia Fox, A. J. et al. (2009) The basic science of articular cartilage: Structure, composition, and function. Sports health. [Online] 1 (6), 461–468.

[3] Bergholt, M. S et al. (2016) Raman Spectroscopy Reveals New Insights into the Zonal Organization of Native and Tissue-Engineered Articular Cartilage. ACS Central Science [Online] DOI: 10.1021/acscentsci.6b00222.

[4] Cong, B. et al. (2023) Current and Novel Therapeutics for Articular Cartilage Repair and Regeneration. Therapeutics and clinical risk management. [Online] 19485–502.

[5] Buckwalter, J.A et al. (2005) Articular cartilage and osteoarthritis. Instructional Course Lectures-American Academy of Orthopaedic Surgeons, 54, p.465.

[6] Kwon, H. et al. (2019) Surgical and tissue engineering strategies for articular cartilage and meniscus repair. Nature reviews. Rheumatology. [Online] 15 (9), 550–570.

[7] Muir, H., 1978. Proteoglycans of cartilage. Journal of Clinical Pathology. Supplement (Royal College of Pathologists)., 12, p.67.

[8] Roughley, P.J. and White, R.J., 1980. Age-related changes in the structure of the proteoglycan subunits from human articular cartilage. Journal of Biological Chemistry, 255(1), pp.217-224.

[9] Mano, J. F. (2013) Biomimetic Approaches for Biomaterials Development. 1st ed. Somerset: John Wiley & Sons, Incorporated.

[10] Bakhtiary N, Liu C, Ghorbani F. Bioactive Inks Development for Osteochondral Tissue Engineering: A Mini-Review. Gels. 2021; 7(4):274. https://doi.org/10.3390/gels7040274

[11] Kiviranta, I. et al. (1985) Microspectrophotometric quantitation of glycosaminoglycans in articular cartilage sections stained with Safranin O. Histochemistry. [Online] 82 (3), 249–255.

[12] Camplejohn, K. L. & Allard, S. A. (1988) Limitations of safranin 'O' staining in proteoglycan-depleted cartilage demonstrated with monoclonal antibodies. Histochemistry. [Online] 89 (2), 185–188.

[13] Kjosness, K. M. et al. (2023) Modified Periodic Acid-Schiff (PAS) Is an Alternative to Safranin O for Discriminating Bone–Cartilage Interfaces. JBMR plus. [Online] 7 (6), e10742–n/a.

[14] Mansour, J.M., 2003. Biomechanics of cartilage. Kinesiology: the mechanics and pathomechanics of human movement, 2, pp.66-79.

[15] Torzilli, P.A., Arduino, J.M., Gregory, J.D. and Bansal, M., 1997. Effect of proteoglycan removal on solute mobility in articular cartilage. Journal of biomechanics, 30(9), pp.895-902.

[16] Mankin, H.J. et al. (1981) Biochemical and metabolic abnormalities in articular cartilage from osteoarthritic human hips. III. Distribution and metabolism of amino sugar-containing macromolecules. JBJS, 63(1), pp.131-139.

[17] Van der Sluijs, J. A. et al. (1992) The reliability of the Mankin score for osteoarthritis. Journal of orthopaedic research. [Online] 10 (1), 58–61.

[18] Mehta, S.B. et al., R.,(2013) Polarized light imaging of birefringence and diattenuation at high resolution and high sensitivity. Journal of Optics, 15(9), p.094007.

[19] Rieppo, J. et al. (2008) Practical considerations in the use of polarized light microscopy in the analysis of the collagen network in articular cartilage. Microscopy research and technique, 71(4), pp.279-287.

[20] Rieppo, J. et al. (2008) Practical considerations in the use of polarized light microscopy in the analysis of the collagen network in articular cartilage. Microscopy research and technique. [Online] 71 (4), 279–287.